13th ewtec 2019 Proceedings of the 13th European Wave and Tidal Energy Conference 1-6 Sept 2019, Naples, Italy

Performance assessment of different RANS turbulence models in numerical simulations for BH-OWSC

Duy Tong Nguyen, Yi-Chih Chow, Jiahn-Horng Chen, and Chen-Chou Lin

Abstract—**Ocean wave energy has attracted many attentions from researchers and developers mainly because of its great energy potential. In order to capture and transform wave energy, the Wave Energy Converter (WEC) has to be designed and developed. The Bottom-Hinged Oscillating Wave Surge Converter (BH-OWSC) is a pitching device that extracts wave energy mainly in the surge direction. For regions like Taiwan where wave resources are at low to median levels and weathers have extreme events like typhoon, the BH-OWSC seems to be the most appropriate choice for the development of wave energy. This paper reports a performance assessment of three widely-used Reynolds Averaged Navier-Stokes (RANS) turbulence models, along with the laminar flow model, incorporated in the numerical simulations for the BH-OWSC. These turbulence models are the standard k-ε model, the Renormalized Group (RNG) k-ε model, and the k-ω model. The dimensions of the BH-OWSC model, the incoming wave conditions and the damping coefficient of the Power Take-Off (PTO) used in the numerical simulations are identical to that of a previous experiment. The numerical results regarding the capture factor, and the angular crest, angular trough and angular stroke of the pitching motion are compared against that of the data measured in the experiment. In general, all the numerical results presented in this paper appear quite in agreement with the experimental data, featuring the almost identical and best performances with the k-ω and laminar flow models.**

Keywords— **BH-OWSC, RANS turbulence models, capture factor, angular stroke.**

I. Introduction

ESTIMATED by the World Energy Council in 2016, the ocean waves all over the world have total energy potential of 32 PWh/yr according [1], almost double that of the global electricity supply in 2008 (17 PWh/yr). So the ocean wave energy arguably holds the highest potential globally among all the forms of renewable energy. Therefore, the need to develop the device for harvesting ocean wave energy, the WEC (Wave Energy Converter), has inspired the largest number of patents published globally in the field of ocean energy. According to the EMEC (European Marine Energy Centre), WECs can be categorized into 8 types: Attenuator, Point Absorber (PA), Overtopping, Pressure Differential, Oscillating Wave Surge Converter (OWSC), Bulge Wave, Rotating Mass and Oscillating Water Column (OWC). For the medium wave resources as many regions in Asia enjoy, the WEC's wave-capturing performance is especially important. Several research works, e.g. Renzi and Dias [2] and Chow et al. [3], have found that the OWSC is capable of achieving performance with high capture factor, which can be even higher than 1 for the OWSC at resonant conditions. In addition, the prime mover of the Bottom-Hinged OWSC (BH-OWSC) can be folded onto the seabed in order to avoid huge impacts from large waves during extreme weathers like typhoon to increase its survivability. As a result, the present paper chooses BH-OWSC as the research target for Computational Fluid Dynamics (CFD) efforts.

Many previous works have shown that CFD is an effective tool for analyzing WEC problems. For instance, Wolgamot et al. [4] presented detailed descriptions and comparisons of different numerical models for simulating the hydrodynamics associated with WECs. They showed that the conventional CFD effort appears ideally suited to the OWC problem. And Devolder et al. [5] achieved a stable fluid-structure-coupled solver for simulating arrays of two, five and nine floating PAs and accurately predicted their individual motions. Bhinder et al. [6] also supported that the CFD has shown its effectiveness in capturing flow non-linearities such as viscous effects, vortical structures

Paper ID: 1519, Track: WHM. This work was supported by the Ministry of Science and Technology of Taiwan under the grant number: MOST 107-2221-E-019 -054 -MY2.

D. T. Nguyen is Ph.D. student with Department of Systems Engineering and Naval Architecture, National Taiwan Ocean University (NTOU), Keelung, 20224, Taiwan, R.O.C. (e-mail: 10551033@email.ntou.edu.tw)

Y. C. Chow, 1st corresponding author, is Associate Professor with Department of Systems Engineering and Naval Architecture, and Deputy Director of Center for Ocean Energy System (COES), NTOU, Keelung, 20224, Taiwan, R.O.C. (e-mail: ycchow@email.ntou.edu.tw)

J. H. Chen is Professor with Department of Systems Engineering and Naval Architecture, and COES, NTOU, Keelung, 20224, Taiwan, R.O.C. (e-mail: B0105@mail.ntou.edu.tw)

C. C. Lin, 2nd corresponding author, is Professor with Department of Mechanical and Mechatronic Engineering, and Director of COES, NTOU, Keelung, 20224, Taiwan, R.O.C. (e-mail: cclin@mail.ntou.edu.tw).

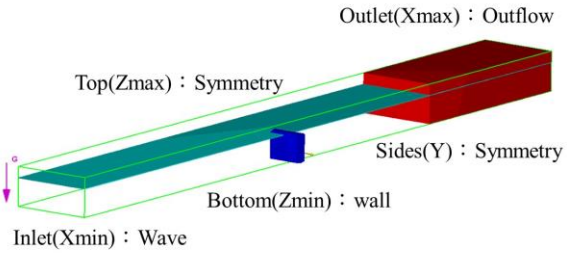

Fig. 1. Computation domain and boundary conditions

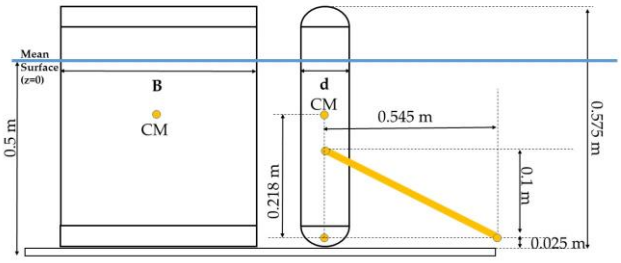

Fig. 2. Schematic of the BH-OWSC's flap geometry.

and turbulence phenomena to a certain extent. Another example is Olivia et al. [7] who used three Reynolds Averaged Navier-Stokes (RANS) solvers to calculate the radiation damping coefficients associated with certain WECs and they claimed that the accuracy of solving the diffraction-radiation problem is improved. The BH-OWSC has also become a popular target for CFD researches, e.g. Rafiee et al. [8]. Certain success in simulating the BH-OWSC has been achieved. For instance, Wei et al. [9] used a commercial CFD package to deal with viscous effects on the performance of BH-OWSC under normal operating conditions. Their numerical results of wave dynamics, pitching motion of the flap and pressure distribution on the flap showed good agreements with the experimental data of a 1:25 scale model test conducted in a wave tank. From these previous research results, it seems that numerical modelling has become the most effective tool to be used in the processes of WECs' design and development.

As pointed out by Mingham et al. [10], however, the fact that the complexity of turbulence results complicated and highly problem-dependent turbulence models causes issues with the accuracy and applicability of a turbulence model used in the RANS simulation for a WEC such as the BH-OWSC. Therefore, this paper conducts a performance assessment of three widely-used RANS turbulence models, along with the laminar flow model, incorporated in the numerical simulations for the BH-OWSC using the CFD software package FLOW-3D. These three turbulence models are the standard k-ε model, the Renormalized Group (RNG) k-ε model, and the k-ω model. We adopt for the CFD work the dimensions of the BH-OWSC model, the incoming wave conditions and the damping coefficient of the Power Take-Off (PTO) from a previous experiment performed by Chow et al. [11]. And the CFD results of capture factor and angular strokes of the BH-OWSC are compared with that of the experimental data obtained from the same experiment, shedding light on the best model one can choose for simulating the BH-OWSC operated in the typical wave climate of Taiwan.

II. NUMERICAL MODELLING

BH-OWSC, generally regarded as one class of nearshore WECs, exploits the horizontal fluid particle movement of waves, and oscillates in the surge direction as opposed to the heaving devices deployed in the deeper water [12]. Typical examples of the BH-OWSC are the WaveRoller, a commercial WEC developed by AW-Energy Oy, and the Oyster 800 developed by Aquamarine Power.

The energy adsorption performance of the BH-OWSC is assessed using the RANS-based CFD software, FLOW3D, in which the free surface flow problems can be well modelled using the volume of fluid (VOF) scheme. The numerical model in this study was based on the experiments undertaken by Chow et al. [11], in which the 1/20th scaled flap model of Oyster and wave conditions of the northeastern coastal water of Taiwan were adopted. Three different turbulence models, i.e., the standard k-ε model, the RNG k-ε model, and the k-ω model, along with the laminar model are used in the computation for comparison. The following context describes the numerical model setups. The computer hardware used in this simulation was Intel(R) core(TM) I7-7740X @4.30GHz, Ram64 GB.

A. Wave basin

Figure 1 shows the rectangular-volume computational domain and boundaries, with the flap model inside. The origin of the domain's coordinate system is set at the geometric center of the rectangular volume. The computational domain is 16 meters long (X-direction: from the inlet to outlet), 2 meters wide (Y-direction), and 1 meter high (Z-direction: upward), whose dimension is based on the actual wave basin size at the Hydraulics Laboratory of the Department of Harbor and River Engineering, National Taiwan Ocean University. The water depth is 0.5 m. A wave absorbing component is added in front of the outflow boundary to avoid the reflected wave from affecting the flap's motion to maintain a steady fluid volume in the computation domain. Due to the symmetry condition, the numerical simulations are performed with respect to one half of the computation domain. A "Wave" boundary condition is applied to the upstream (Xmin = -8 m), whilst an "Outflow" boundary condition to the

TABLE I
BOUNDARY CONDITIONS

Description	Boundary type	Location
X_{max}	Outflow	X = 8 m
X_{min}	Wave	X = -8 m
Y_{max}	Symmetry	Y = 1 m
Y_{min}	Symmetry	Y = 0 m
Z_{max}	Symmetry	Z = 0.5 m
Z_{min}	Wall	Z = -0.5 m

downstream (Xmax = 8 m). The boundary conditions at the wave basin's sidewalls are set as the "Symmetry" for reducing friction effects. The boundary condition at the seabed (Zmin = -0.5 m) is set as no-slip "Wall" condition, whilst at the top (Z= 0.5 m) is set as the symmetry boundary for reducing the effects of surface tension. Hence the boundary conditions are summarized in TABLE I.

B. *Flap model*

As mentioned above, the purpose of the numerical simulation is to compare with the previous experimental results. Thus all dimensions of the flap's numerical model correspond to the actual size the tested model. As shown in Fig. 2, the width, height, and thickness of the flap are 0.5 m, 0.575 m and 0.1 m, respectively. The flap mass is set at 15.51 kg, with the center of mass located at 0.218 m above the hinge, and the hinge set at 0.025 m above the seabed (foundation) to prevent the flap from interfering the seabed during the oscillating pitch motion. In the experiment, two identical hydraulic pumps installed at two lateral ends of the flap were taken as the PTO system. In the numerical simulation, we substitute the pumps with a compression/extension type spring with zero stiffness and designated linear damping coefficient located on the central plane (XZ plane), connecting the two points at the flap and the seabed, as shown in Fig. 2.

C. *Meshing and initial conditions*

FLOW-3D uses a multi-block grid structure, each block has its mesh size, and the grid setting can be either adjacent or nested type. In this study, the nested mesh type is chosen because it is more convenient for finer meshing in the local flap motion area. To get a more accurate numerical simulation result, meshing with two blocks is

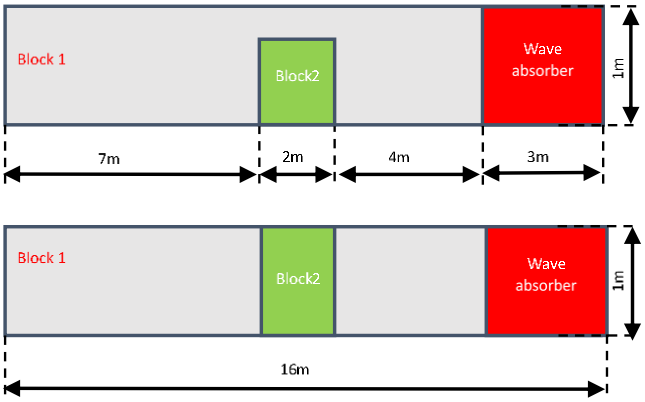

Fig. 3. Schematic of the block arrangement (upper: top view, lower: side view).

adopted; one is the wave area block (block 1), the other is the flap-motion block (block 2), as shown in Fig. 3. Block 1 contains the whole computational domain, whereas block 2 encompasses the flap and its surrounding motion area, of which dimension is 2 m x 0.6 m x 1 m, and the mesh cell size of block 2 is half as that of block 1.

The numerical errors and computation time usually vary significantly from different mesh sizes. Hence, the convergence test is conducted to find a proper mesh setting. Four tests are performed for four different mesh cell sizes of block 2, that is, 0.015 m, 0.03 m, 0.04 m, and 0.06 m for the standard k-ε model. The results are then compared with the experimental data. Finally, we choose the mesh cell size of 0.03 m (for block 2) due to its smallest error compared with errors of other models, as shown in TABLE II. In all simulations of the study, viscous and incompressible fluid with a density of 1000 kg/m^3, the PTO's damping coefficient of 1401.5 Ns/m, and zero spring constant were applied. During the numerical simulations, an appropriate time of 60 s was chosen to extracts the results, and the initial time step was set to be 0.01 s.

D. *Model validation*

To choose the best numerical model of BH-OWSC for comparing with the existing experimental data, we conduct the simulations using four different models, namely, the laminar model, the standard k-ε model, the RNG k-ε model, and the k-ω model. The numerical model is validated by comparing the numerical results of an isolated flap (flapper 2) from Chow et al. [11]. The comparisons cover four aspects: capture factor (CF),

TABLE II
MESH SIZE TEST

Test No.	Block 1 mesh size	Block 2 mesh size	Cell counts	Elapsed time	Strokes (degree)	Error
1	0.03	0.015	1063085	2 h:51min:21 s	12.23	0.43%
2	0.06	0.03	154631	9 min: 29 s	11.94	0.14%
3	0.08	0.04	71700	3 min: 34 s	12.04	0.24%
4	0.12	0.06	22645	2 min: 18 s	13.80	2.00%

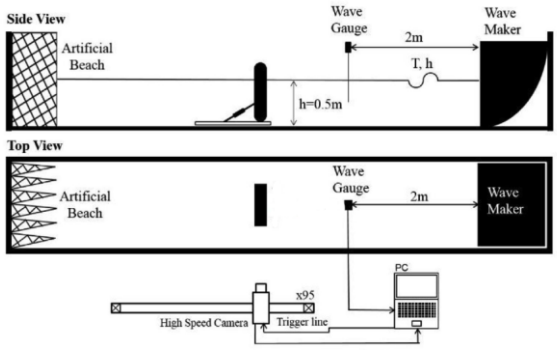

Fig. 4. Schematic of experimental setup for the operation of a single BH-OWSC in isolation [11]

angular crests (θ+), troughs (θ-), and strokes (θs). Also, the elapsed time of a simulation process can be taken as a criterion for choosing the best numerical model.

1) Wave dynamics

The wave condition used in the simulation is the linear wave with a wave height of 0.07 m, a wave period of 1.56 s, and the calculated wavelength of 2.97 m. These characteristic wave conditions are adopted and scaled down from the wave data of northeast coastal waters of Taiwan.

2) Flap rotation

The rotations of flap for four numerical models from the FLOW3D simulation results are compared with the experimental data. As mentioned previously, the damping coefficient is given at a constant value of 1401.5 Ns/m. FLOW3D results also show the length of extension from compression and extension spring.

According to Chow et al. [3], the energy extracted by the PTO can be calculated by

$$P_{PTO} = C_{PTO} V_{PTO}^2 \tag{1}$$

Where C_{PTO} is the damping coefficient, V_{PTO} is the relative velocity of PTO calculated from length extension of spring.

The following formulation gives the incident wave power:

$$P_{wave} = \frac{1}{8} \rho g H^3 C g \tag{2}$$

Finally, the capture factor of OWSC is derived by

$$\mathrm{CF} = \frac{P_{PTO}}{B \times P_{wave}} \tag{3}$$

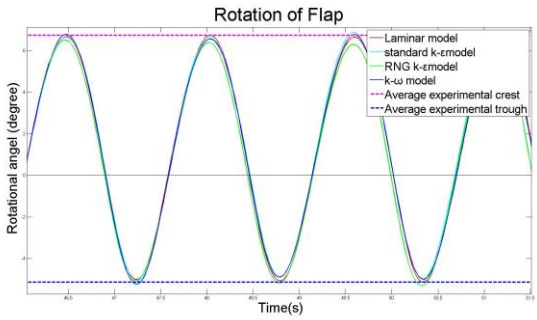

Fig. 5. Angular crests (θ+), troughs (θ-) and strokes (θs) of flap compared to experimental data.

E. Experiment

Chow et al. [11] have done experiments for operations of a single BH-OWSC in isolation and double BH-OWSCs in tandem. For the purpose of this study, we choose only the data from the operation of a single BH-OWSC in isolation to compare with the numerical simulations. As shown in Fig. 4, the experiment was performed in a wave channel with dimensions of 16 m long, 2 m wide and 1 m high. The wave maker on one end of the channel was manufactured by the Edinburgh Designs and an effective wave absorber on the other end was installed. The water depth in the experiment was kept at 0.5 m.

The flap panel, having dimensions of 0.5 m wide , 0.575 m high and 0.1 m thick, was located at the middle of the channel. The density of the flap was 555 kg/m^3, the buoyancy centre height was 0.220 m, and the mass centre high was 0.218 m. There were two hydraulic pumps individually on the sides of the flap as the PTO. The incident wave in this experiment was a linear wave with period of 1.56 s (wave length of 2.97 m) and height of 0.07 m.

Time-series images of the pitching BH-OWSC were acquired by a high-speed camera at the sample rate of 100 frames/s. The duration of wave generation was 60 s. The data of several wave periods were taken after the incident wave was well developed and before the flap motion was significantly affected by the wave reflections from the boundary.

III. RESULTS

As mentioned before, these numerical simulations of BH-OWSC are intended to find the most effective flow model which delivers results closest to that of the experiment, based on the four parameters: capture factor (CF), angular crests (θ+), troughs (θ-), and strokes (θs). These parameters resulting from four flow models will be compared with the experimental data. The comparisons are detailed as follows.

Firstly, among three widely-used RANS turbulence models, the k-ω model delivers results closest to the experimental data. As shown in Table III, the CF due to the k-ω model (0.546) is smaller and closer to the experimental

TABLE III
NUMERICAL RESULTS

Test No.	Numerical model	Capture factor (CF)	Trough (θ-)	Crest (θ+)	Stroke (θs)	Elapsed time
1	Laminar	0.547	-5.07	6.76	11.83	8 min: 58 s
2	Standard k-ε	0.553	-5.26	6.68	11.94	9 min: 29 s
3	RNG k-ε	0.620	-5.86	6.40	12.26	9 min: 44 s
4	k-ω	0.546	-5.36	6.48	11.84	10 min: 6 s
5	**Experiment [11]**	**0.530**	**-5.15**	**6.73**	**11.88**	**N/A**

data (0.530) than that due to the standard k-ε model (0.553) and the RNG k-ε model (0.620). We also find the similar trend in the angular stroke (θs) of the flap: θs due to the k-ω model (11.84 degrees) is closer to the experimental data (11.88 degrees) than that due to the standard k-ε model (11.94 degrees) and the RNG k-ε model (12.26 degrees).

Secondly, the laminar model and the k-ω model deliver parameters close to each other, i.e. the results due to the laminar model are very close to the experimental data as well. For example, as shown in Table III, the laminar model and the k-ω model result in the CFs of 0.547 and 0.546, respectively, and they are very close to the experimental CF (0.530). Figure 5 shows the variations of the flapping angle with time due to the four flow models. Combined with Table III, the angular crests (θ+) and troughs (θ-) due to the laminar model are closet to the experimental data. In general, all the numerical results are in good agreement with the experimental data.

Table III also shows the elapsed time for completing a simulation with a specific flow model. As expected, the case with the laminar model took the shortest time (8 min: 58 s). And the case with the k-ω model took the longest time (10 min: 6 s), while the other two cases took 9 min: 29 s for the standard k-ε model and 9 min: 44 s for the RNG k-ε model. Using the case with the standard k-ε model as the base, the elapsed time for the case with the k-ω model is 6.5% longer while the CF and θs for the case with the k-ω model are 1.3% and 0.2% closer to that of the experiment, respectively. Using the case with the RNG k-ε model as the base, the elapsed time for the case with the k-ω model is only 3.8% longer while the CF and θs for the case with the k-ω model are 14.0% and 2.9% closer to that of the experiment, respectively. Therefore, among the cases with the three turbulence models, the k-ω model appears the most accurate while the standard k-ε model appears the most efficient.

IV. CONCLUSION

We have successfully conducted CFD simulations for a previous BH-OWSC experiment with three widely-used RANS turbulence models, i.e. the standard k-ε model, the Renormalized Group (RNG) k-ε model, and the k-ω model, and the laminar flow model. The numerical results of the integral performances of the BH-OWSC model, i.e. the capture factor (CF), angular crest (θ+), angular trough (θ-) and angular stroke (θs), are compared against that of the data measured in the experiment in order for us to assess the performances with these four models incorporated in CFD simulations for a BH-OWSC operated in the typical wave climate of Taiwan.

In general, all the numerical results presented in this paper appear in quite good agreement with the experimental data, even for the results with the laminar flow model. Along with the fact that the angular stroke of the pitching BH-OWSC is only around 12 degrees, it seems to suggest that the state of the flow around the BH-OWSC model is at least sometimes laminar, if not always laminar. Among the results with the three turbulence models, the capture factor and the angular stroke with the k-ω model are the closest to that of the experiment and almost identical to that with the laminar flow case, whereas the capture factor and the angular stroke with the RNG k-ε model deviate the most. In the comparison of the angular troughs and crests, it clearly shows that the results with the laminar flow model are the best predictions among all the numerical results. It further supports our previous speculation that the flow state around the BH-OWSC model is at least sometimes laminar. However, this point can only be validated with future experimental data of flow measurement. Nevertheless, the flow state around the BH-OWSC will most likely turn to be turbulent when the device is operating close to its resonance or under large waves, i.e. the laminar flow model most likely loses its applicability in these situations.

Among the cases with the three turbulence models, the k-ω model appears the most accurate while the standard k-ε model appears the most efficient. However, the elapsed time for the case with the k-ω model is only 6.5% longer than that for the case with the standard k-ε model. As a result, we will choose to use the k-ω model in the RANS simulations for the BH-OWSC in the future.

REFERENCES

[1] World energy council, "World energy resources 2016", October 2016.[Online]. Available: https://www.worldenergy.org/wp-content/uploads/2016/10/World-Energy-Resources-Full-report-2016.10.03.pdf

[2] E. Renzi, F. Dias, "Hydrodynamics of the oscillating wave surge converter in the open ocean", *Eur. J. Mech. B/Fluids, Vol.41*, 2013, p.1-10.
[3] Y.C. Chow, Y.C. Chang, D.W. Chen, C.C. Lin, and S.Y. Tzang, "Parametric Design Methodology for Maximizing Energy Capture of a Bottom-Hinged Flap-Type WEC with Medium Wave Resources," *Renewable Energy,* Vol.126, October 2018, p. 605-616.
[4] H.A. Wolgamot; C.J. Fitzgerald, "Nonlinear hydrodynamic and real fluid effects on wave energy converters," *Proc. Inst. Mech. Eng. Part A J. Power Energy 2015,* 229, 772–794.
[5] Brecht Devolder, Vasiliki Stratigaki, Peter Troch and Pieter Rauwoens, "CFD Simulations of Floating Point Absorber Wave Energy Converter Arrays Subjected to Regular Waves," *Energies 2018,11(3), 641,* DOI:10.3390/en11030641, [Online].
[6] Majid A. Bhinder, M.T. Rahmati, C.G. Mingham, G.A. Aggidis, "Numerical hydrodynamic modelling of a pitching wave energy converter," *European Journal of Computational Mechanics*, vol.24, 2015 - Issue 4, p.129-143.
[7] Olivia Thilleul, Aurélien Babarit, Aurélien Drouet, Sébastien Le Floch, "Validation of CFD for the Determination of Damping Coefficients for the Use of Wave Energy Converters Modelling", in *ASME 2013 32nd International Conference on Ocean, Offshore and Arctic Engineering Cite*, Nantes, France, Vol.3, 2013, DOI: 10.1115/OMAE2013-10818.
[8] Ashkan Rafiee, Björn Elsäßer, "Numerical simulation of wave interaction with an Oscillating Wave Surge Converter," *ASME 2013 32nd International Conference on Ocean, Offshore and Arctic Engineering,* Nantes, France, Vol.5, 2013, DOI: 10.1115/OMAE2013-10195.
[9] Yanji Wei, Ashkan Rafiee, Alan Henry, Frederic Dias, "Wave interaction with an oscillating wave surge converter, Part I: Viscous effects," *Ocean Engineering,* Vol.104, 2015, p.185–203.
[10] C. Mingham, L. Qian, D. Causon," Numerical Modelling of Wave Energy Converters", edited by Matt Folley, *Academic Press, Elsevier Inc.*, 2016, ch.6. ISBN: 978-0-12-803210-7.
[11] Y.C. Chow, Y.C. Chang, C.C Lin, J.H Chen, S.Y. Tzang, "Experimental Investigations on Two Bottom-Hinged Wave Energy Converters in Tandem Operations at Different Separation Distances," *Ocean Engineering,* Vol.164, 15 September 2018, p.322-331.
[12] Trevor Whittaker, Matt Folley, "Nearshore oscillating wave surge converters and the development of Oyster," *Phil. Trans. R. Soc. A (2012),* 370, p.345–364, DOI: 10.1098/rsta.2011.0152. [Online].